Chemical Engineering Journal 146 (2009) 90–97

Contents lists available at ScienceDirect

Chemical Engineering Journal

journal homepage: www.elsevier.com/locate/cej

Sorption of distillery spent wash onto fly ash: Kinetics and mass transfer studies

R. Krishna Prasad*, S.N. Srivastava

School of Chemical & Biotechnology, SASTRA University, Thanjavur 613 402, India

ARTICLE INFO

Article history:
Received 31 December 2007
Received in revised form 14 May 2008
Accepted 15 May 2008

Keywords:
Adsorption
Fly ash
Kinetics
Mass transfer studies

ABSTRACT

Adsorption studies for sorption of distillery spent wash onto fly ash particles were studied in both batch and packed column. Equilibrium data were fitted to the Sips, Elvoich and Dubinin–Radushkevich, Redlich–Peterson, Langmuir four types and Ho's four types of pseudo-second-order kinetic models. The complete error analysis was done to determine the best isotherm model using six different non-linear error functions: chi-square (χ^2), sum of square errors (SSEs), composite fractional error function (HYBRD), derivative of Marquardt's percent standard deviation (MPSD), average relative error (ARE), sum of absolute errors (EABS) and linear regression correlation coefficient (r^2). The Biot number was determined using internal mass transfer coefficient and the external mass transfer coefficient estimated using Mathews and Weber model and Furusawa and Smith model. The Biot number estimated provides that external film transfer controls the mechanism of sorption of spent wash onto fly ash. Packed column adsorption was analyzed using Thomas model and Adams–Bohart model for different flow rates of studies.

1. Introduction

Molasses spent wash (MSW) from distillation still contains a dark brown recalcitrant pigment called melanoidin formed due to maillard amino-carbonyl reaction. The empirical formula of melanoidin is $C_{17-18}H_{26-27}O_{10}N$. It is a product of non-enzymatic reaction between sugars and amino compounds. The molecular weight distribution is between 5000 and 40,000. It is acidic, polymeric and composed of highly dispersed colloids, which are negatively charged due to the dissociation of carboxylic acids and phenolic groups [1–3].

Several studies have been carried out concerning the decolorization of waste water using cyanobacterium [4], fungi such as aspergillus fumigatus [5], coriolus [6], phanerochaete chrysosporium [7], electro chemical studies [8,9] and studies using various coagulants like aluminum sulfate ($Al_2(SO_4)_3{\cdot}14H_2O$), ferric chloride ($FeCl_3{\cdot}6H_2O$), sodium aluminate, aluminum chloride and ferric sulfate [10–14] have shown to degrade melanoidin and anaerobic mass imparting color to spent wash. However, recent studies have pointed out several serious drawbacks of using aluminum salts, such as Alzheimer's disease [15]. There is also the problem of reaction of alum with natural alkalinity present in the water leading to a reduction of pH [16].

Currently sorption technique is proved to be an effective and attractive process for the wastewater treatment. Also this method will become inexpensive, if the sorbent material used is of cheaper cost and does not require any expensive additional pretreatment step. During coal fired electric power generation, two main types of coal combustion by products are obtained, fly ash and bottom ash. The current annual worldwide production of coal ash is estimated about 700 million tons of which at least 70% is fly ash [17]. Although, significant quantities are being used in a range of applications like substitute for cement in a concrete, however still large amounts are not used and this requires disposal. Making a more productive use of fly ash would have considerable environmental benefits, reducing air and water pollution. The large amount of fly ash discarded in coal fired power stations can be utilized as a good adsorbent for color removal [18–21]. Previously several researchers had proved several low cost materials such as rice husk [22], sugar cane dust [23], bagasse pith [24] were used in color removal. Scrap rubber, peanut husks and composted bark to remove metal ion from wastewater [25,26].

In the present study the equilibrium data of adsorption of spent wash onto fly ash at different temperatures were analyzed with Sips, Elvoich, Dubinin–Radushkevich, Redlich–Peterson and Langmuir four types of isotherms. The sorption was also analyzed using Ho's four types of pseudo-second-order kinetic models. A complete error analysis using six different types of non-linear error functions was done. Mass transfer studies were evaluated to determine external and internal mass transfer coefficients that are used to determine the Biot number. The mechanism of adsorption process was analyzed using the Biot number evaluated. Packed bed adsorption studies were conducted at different flow rates to analyze the results using Thomas model and Adams–Bohart model.

* Corresponding author. Tel.: +91 94434 60815; fax: +91 4362 264120.
E-mail address: rkprasad_cbe@rediffmail.com (R. Krishna Prasad).

1385-8947/$ – see front matter © 2008 Elsevier B.V. All rights reserved.
doi:10.1016/j.cej.2008.05.021

Nomenclature

a	total interfacial area of the particles (cm^2)
a_{LF}	Sips isotherm constant ($L\,mg^{-1}$)
A	Redlich–Peterson isotherm constant ($L\,g^{-1}$)
ARE	average relative error
B	Redlich–Peterson isotherm constant ($L\,mg^{-1}$)
B_N	Biot number
C_{ads}	amount of sorbate sorbed onto sorbent surface ($mg\,g^{-1}$)
C_e	equilibrium concentration in liquid phase ($mg\,L^{-1}$)
C_t	concentration of spent wash solution at time t ($mg\,L^{-1}$)
C_0	initial concentration of spent wash solution ($mg\,L^{-1}$)
d	mean particle diameter (cm)
D	intraparticle diffusion ($cm^2\,min^{-1}$)
E	sorption energy ($KJ\,g^{-1}$)
EABS	sum of absolute errors
g	exponent which lies between 0 and 1
h	initial sorption rate ($mg\,g^{-1}\,min^{-1}$)
HYBRD	composite fractional error function
k_f	initial external mass transfer coefficient ($cm\,min^{-1}$)
k_2	pseudo-second-order rate constant ($g\,mg^{-1}\,min^{-1}$)
K_{AB}	kinetic constant in the Adams–Bohart model (L/(mg min))
K_L	Langmuir adsorption constant ($L\,mg^{-1}$)
K_{Th}	Thomas model constant (L/(mg min))
m_s	concentration of sorbent in liquid phase ($mg\,L^{-1}$)
m_{total}	total amount of solids sent to the column (mg)
M	amount of adsorbent (g)
MPSD	derivative of Marquardt's percent standard deviation
n	Freundlich parameter
N_0	sorption capacity of the bed per unit volume of the bed ($mg\,L^{-1}$)
q_e	equilibrium concentration in solid phase ($mg\,g^{-1}$)
q_m	Langmuir isotherm parameter, maximum spent wash adsorbed/unit mass of adsorbent ($mg\,g^{-1}$)
q_o	amount of spent wash adsorbed at infinite time ($mg\,g^{-1}$)
q_t	amount of spent wash adsorbed per unit mass of adsorbent at time t ($mg\,g^{-1}$)
q_{total}	total adsorbed quantity in the column (mg)
Q	column feed flow rate ($mL\,min^{-1}$)
r^2	linear regression correlation coefficient
R	universal gas constant (8.314 J/mol K)
R_L	Langmuir separation or equilibrium parameter
$\%R_t$	percentage color removal
SSE	sum of square errors
S_a	outer surface area of adsorbent particles per unit volume of particle free slurry (cm^{-1})
t	time (min)
t_{total}	total flow time (min)
T	temperature (K)
U_0	superficial velocity of the solution ($cm\,min^{-1}$)
V	total solution volume (L)
V_{eff}	effluent volume (mL)
X_m	maximum sorption capacity of sorbent ($mg\,g^{-1}$)
Z	bed height (cm)

Greek letters

α	initial adsorption rate ($mg\,g^{-1}\,min^{-1}$)
β	desorption constant ($g\,mg^{-1}$)
γ	sorption energy ($KJ^2\,g^{-2}$)
ε	Polanyi sorption potential
ρ	apparent density of the adsorbent ($g\,mL^{-1}$)
χ^2	chi-square

2. Experimental

2.1. Materials and methods

The distillery spent washes used for the study was collected from a distillery unit near Tiruchi. The sample was diluted to desired dilution using deionized water. The pH of the sample was adjusted using 0.1 M H_2SO_4 or 0.1 M NaOH as required. Table 1 gives the physico-chemical characteristics of raw spent wash that were analyzed as described in standard methods [27].

The fly ash was obtained from Lignite Thermal Power Station. The fly ash was sieved by using a sieve set and then was collected in the range of BSS# −72 + 100, −100 + 150, −150 + 200 and −200 + 300 mesh size. The fly ash was used as received without any pretreatment in the adsorption experiments. Chemical composition of fly ash by chemical analysis was given as SiO_2, 15.14; Fe_2O_3, 3.30; Al_2O_3, 7.82; CaO, 24.66; MgO, 4.5; SO_3, 14.22; K_2O, 0.28; Na_2O, 0.57; TiO_2, 1.03 and loss on ignition, 2.31 wt%.

Batch adsorption studies were conducted at three different temperatures (293 K, 303 K and 313 K). In each experiment accurately weighed fly ash was added to 100 mL of distillery spent wash solution taken in a 250 mL conical flask and the mixture was agitated at 200 rpm in an incubated shaker at constant temperature for 3 h. The analysis of sample was done after filtering it using Whatmann 42 filter paper. Concentrations of the filtered samples were determined from the absorbance of the solution at the characteristic wavelength 475 nm using a double beam UV–vis spectrophotometer (Systronics 2201) [28,2]. The readings were taken in duplicate for each individual solution to check repeatability and the average of the values were taken.

Percentage color removal (R_t) was calculated using the formula

$$\%R_t = \frac{C_0 - C_t}{C_0} 100 \quad (1)$$

Specific uptake was calculated by

$$q_t = \frac{C_0 - C_t}{m_s} \quad (2)$$

Bulk removal of spent wash onto fly ash was investigated using packed bed of BSS# −100 + 150 mesh size fly ash particles. Glass column with internal diameter 2 cm, fitted with five sampling points at 5 cm intervals, was used for the study. At the bottom of the packing 2 cm high layer of glass beads (3 mm diameter) was used to

Table 1
Physico-chemical characteristics of distillery spent wash (10% diluted)

Parameters	Magnitude
pH	4.2–4.3
Temperature (°C)	30
Color	Dark brown
Odor	Burnt sugar
Chemical oxygen demand ($mg\,L^{-1}$)	10,000–11,000
Biochemical oxygen demand ($mg\,L^{-1}$)	7000–7500
Total dissolved solids ($mg\,L^{-1}$)	5500–5700
Chloride ($mg\,L^{-1}$)	500–600
Potassium ($mg\,L^{-1}$)	1000–1300
Calcium ($mg\,L^{-1}$)	210–300

Table 2
Values of error functions for different isotherms for sorption of spent wash onto fly ash at 303 K

Isotherm	Chi-square	SSE	HYBRD	MPSD	ARE	EABS
Sips	0.0102	0.3411	0.0103	0.0003	0.0299	0.9820
Elvoich	11.4311	527.8273	7.76344	0.1149	0.4501	29.4737
Dubinin–Radushkevich	1.1549	86.1247	1.2494	0.0186	0.2173	14.5718
Redlich–Peterson	0.3811	27.7689	0.4021	0.0067	0.1419	8.2446
Ho—type 1	0.1152	8.0968	0.1179	0.0021	0.0914	5.0962
Ho—type 2	1.4162	108.4844	1.5345	0.0251	0.3146	18.4457
Ho—type 3	1.4831	114.0005	1.6099	0.0685	0.3227	18.8988
Ho—type 4	1.8831	148.2431	2.0659	0.0338	0.3662	21.4011
Langmuir—type 1	2.8003	100.6351	2.5012	0.0797	0.4994	19.8036
Langmuir—type 2	4.5240	315.8312	4.0306	0.0562	0.3473	23.9759
Langmuir—type 3	3.1815	216.6781	3.1889	0.0530	0.3934	23.6889
Langmuir—type 4	2.6352	164.8306	2.7778	0.0557	0.4426	23.2631

provide uniform inlet flow to the column. Distillery spent wash solution was introduced into the column at desired flow rate using a peristaltic pump. The experiments were conducted for three different flow rates (1 L/h, 2 L/h and 3 L/h) at 10 cm bed height using distillery spent wash of pH 7. The initial concentration of distillery spent wash used is 2000 mg L^{-1} for 5% dilution spent wash. Samples were collected at regular intervals from all the sampling points. The performance of packed column is described through the concept of the breakthrough curve, which is the plot of time versus effluent concentration curve.

3. Results and discussions

3.1. Adsorption isotherms

The prediction of batch sorption kinetics is necessary for the design of industrial sorption columns. The nature of the sorption process will depend on physical or chemical characteristics of the adsorbent system and also on the system conditions. The results of the studies conducted were analyzed using five different isotherm models. Six different non-linear error functions χ^2, SSE, HYBRD, MPSD, ARE, EABS and linear error function r^2 were employed to find out the most suitable isotherm models. Definition of these error functions was described elsewhere [29,30]. The fitness of isotherm to the experimental equilibrium data was further analyzed using various non-linear error functions: χ^2, SSE, HYBRD, MPSD, ARE and EABS. The values of error functions for different isotherms are given in Table 2.

Table 3
Sips isotherm constants for the sorption of spent wash onto fly ash at different temperatures using non-linear method

Temperature (K)	Sips isotherm constants			
	q_m (mg g^{-1})	a_{LF} (L mg^{-1})	n	r^2
293	0.7718	1.2693	0.4798	0.9976
303	0.5780	1.1000	0.4911	0.9999
313	0.2147	0.7682	0.5346	0.9986

3.2. Sips isotherm

Sips isotherm (or some times known as Langmuir–Freundlich equation) is employed to analyze the equilibrium data obtained during batch studies at three different temperatures (293 K, 303 K and 313 K). It is expressed as [31]

$$q_e = \frac{q_m (a_{LF} C_e)^n}{1 + (a_{LF} C_e) n} \quad (3)$$

Sips isotherm equation is characterized by the heterogeneity factor, n, and it can be employed to describe the heterogenous system. Therefore the Sips isotherm is used to describe the equilibrium of the sorption of distillery spent wash onto fly ash. The evaluated isotherm parameters using non-linear method estimated from Curve Expert 1.3 is tabulated in Table 3. The correlation coefficent, r^2 is 0.999 indicates best fit to the experimental data obtained. The χ^2 value is 0.0102 and other non-linear error functions are less, hence the Sips model is considered to represent the equilbrium data of adsorption.

3.3. Elvoich isotherm

The Elvoich model equation is generally expressed as

$$\frac{dq_t}{dt} = \alpha \exp(-\beta q_t) \quad (4)$$

To simplify the Elvoich equation, Chien and Clayton [32,33] assumed $\alpha\beta t > t$ and by applying the boundary conditions $q_t = 0$ at $t = 0$ and $q_t = q_t$ at $t = t$. Eq. (4) becomes

$$q_t = \frac{\ln \alpha\beta}{\beta} + \frac{1}{\beta} \ln t \quad (5)$$

The plot of q_t versus $\ln t$ should yield a linear relationship with a slope $1/\beta$ and an intercept of $1/\beta \ln(\alpha\beta)$. The Elvoich isotherm parameters estimated at different temperatures at different dilutions studied were given in Table 4. The non-linear error functions are large (SSE is 526, χ^2 is 11.4311), hence this model does not represents the data of sorption studies accurately.

Table 4
Elvoich isotherm constants for the sorption of spent wash onto fly ash at different temperatures

Initial dilution (%)	293 K			303 K			313 K		
	α (mg g^{-1} min^{-1})	β (g mg^{-1})	r^2	α (mg g^{-1} min^{-1})	β (g mg^{-1})	r^2	α (mg g^{-1} min^{-1})	β (g mg^{-1})	r^2
5	63.808	0.4395	0.971	34.065	0.4074	0.975	51.404	0.4573	0.964
10	704.398	0.2056	0.973	544.666	0.2078	0.975	361.970	0.2064	0.958
15	254.968	0.1196	0.966	115.880	0.1099	0.973	68.260	0.1042	0.894
20	487.143	0.093	0.957	440.550	0.0955	0.962	204.789	0.0912	0.958

Table 5
Dubinin–Radushkevich isotherm constants for the sorption of spent wash onto fly ash at different temperatures

Temperature (K)	Dubinin–Radushkevich isotherm constants			
	X_m (mg g^{-1})	β ($\times 10^{-5}$ g mg^{-1})	$-E$ (KJ g^{-1})	r^2
293	141.976	4.209	3.446	0.9886
303	134.164	4.532	3.321	0.9892
313	170.163	7.258	2.624	0.9971

3.4. Dubinin–Radushkevich isotherm

Dubinin–Radushkevich isotherm model is applied to the sorption data in the following linearized form [34]:

$$\ln C_{ads} = \ln X_m - \beta\varepsilon^2 \quad (6)$$

$$\varepsilon = RT \ln \frac{C_0}{C_e} \quad (7)$$

The Polanyi sorption theory [35] postulates fixed volume of sorption sites close to the sorbent surface and existence of sorption potential over these sites. Polanyi sorption potential is the work required to remove a molecule to infinity from its location in the sorption space. This model assumes the heterogeneity of sorption energies within this space. The plot of $\ln C_{ads}$ versus ε^2 is a straight line with coefficient of determination r^2 0.99. The value of sorption energy, E can be correlated to β using the following relationship [36]:

$$E = \frac{1}{(-2\beta)^{0.5}} \quad (8)$$

The isotherm parameters of Dubinin–Radushkevich model were given in Table 5. The sorption energy is negative confirms that sorption of spent wash onto fly ash is an exothermic process. The r^2 values of this isotherm at different temperatures were above 0.988 indicates that the isotherm can be used to define the experimental data. However, non-linear error functions calculated provides larger sum of square error (86.1247) compared to 0.3411 of Sips isotherm. Hence Dubnin–Radushkevich isotherm was not considered as best fit model to describe the experimental data.

3.5. Redlich–Peterson isotherm

The Redlich–Peterson isotherms has three parameters featuring both the Freundlich and Langmuir isotherm equations. It can be described as [37]

$$q_e = \frac{AC_e}{1 + BC_e^g} \quad (9)$$

It has two limiting cases, which can be explained as follows.

When the exponent $g = 1$, the Langmuir equation results, given by

$$q_e = \frac{AC_e}{1 + BC_e} \quad (10)$$

Table 6
Redlich–Peterson isotherm constants for the sorption of spent wash onto fly ash at different temperatures using non-linear method

Temperature (K)	Redlich–Peterson isotherm constants			
	A (L g^{-1})	B (L mg^{-1})	g	r^2
293	6.8430	3.2992	0.5250	0.9976
303	1.9437	1.0374	0.5226	0.9999
313	0.1822	0.0545	0.5901	0.9997

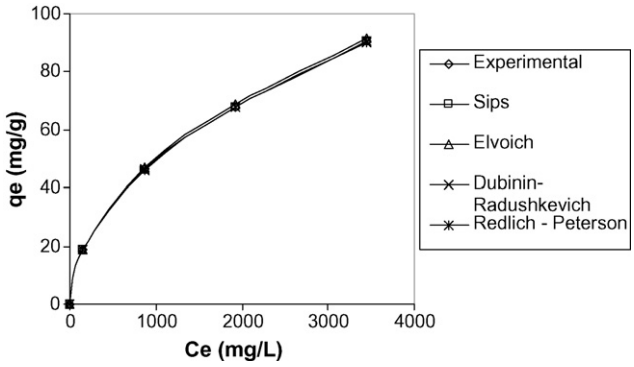

Fig. 1. Equilibrium curves for sorption of spent wash onto fly ash (*conditions*: pH 7, dosage = 10 g, temperature = 303 K, particle size BSS# −100 + 150).

when $g = 0$. Redlich–Peterson isotherm equation transforms to Henry's law equation

$$q_e = \frac{AC_e}{1 + B} \quad (11)$$

Eq. (9) can be can be rearranged as follows:

$$A\frac{C_e}{q_e} - 1 = BC_e^g \quad (12)$$

Eq. (12) can be transformed to a linear equation as follows:

$$\ln\left(A\frac{C_e}{q_e} - 1\right) = \ln B + g \ln C_e \quad (13)$$

The equation has three unknowns A, B and g. It is solved by non-linear method, a trial and error procedure, which is applicable to computer operation using Curve Expert 1.3 software. The results of isotherm parameters are given in Table 6. The value of correlation coefficient r^2 is 0.999 and non-linear error functions are less hence considered as best fit model to describe the experimental equilibrium data for sorption of distillery spent wash onto fly ash. Fig. 1 represents the equilibrium data for Sips, Elvoich, Dubinin–Radushkevich and Redlich–Peterson isotherm equation.

3.6. Ho's pseudo-second-order isotherms—four types

An expression of the pseudo-second-order rate based on the solid capacity has been presented for the kinetics of sorption of spent wash onto fly ash [38,39]:

$$q_t = \frac{q_e^2 k_2 t}{1 + q_e k_2 t} \quad (14)$$

Eq. (14) can be rearranged to obtain

$$q_t = \frac{t}{(1/k_2 q_e^2) + (t/q_e)} \quad (15)$$

In order to distinguish the kinetics equation based on the concentration of a solution from the sorption capacity of solids, this second-order rate equation has been called a pseudo-second-order rate. The pseudo-second-order can be linearized in four different types as given in Table 7. The most popular linear form used is type 1.

Fig. 2 represents the equilibrium data for four types of Ho's pseudo-second-order isotherm. The pseudo-second-order parameters and respective correlation coefficient is given in Table 8. The equilibrium data obtained were analyzed using six non-linear functions that provided low values of error functions for type 1 Ho's kinetics. The correlation coefficient r^2 for type 1 is 0.999 at all temperatures and the error functions are low indicating that the model fits the data obtained by sorption.

Table 7
Pseudo-second-order kinetic model linear forms

Type	Linear form	Plot	Parameters
Type 1	$\frac{t}{q_t} = \frac{1}{k_2 q_e^2} + \frac{1}{q_e} t$	t/q_t vs. t	q_e = 1/slope; k_2 = slope^2/intercept; h = 1/intercept
Type 2	$\frac{1}{q_t} = \left(\frac{1}{k_2 q_e^2}\right) \frac{1}{t} + \frac{1}{q_e}$	$1/q_t$ vs. $1/t$	q_e = 1/intercept; k_2 = intercept^2/slope; h = 1/slope
Type 3	$q_t = q_e - \left(\frac{1}{k_2 q_e}\right) \frac{q_t}{t}$	q_t vs. q_t/t	q_e = intercept; $k_2 = -1/$(intercept × slope); $h = -$intercept/slope
Type 4	$\frac{q_t}{t} = k_2 q_e^2 - k_2 q_e q_t$	q_t/t vs. q_t	$q_e = -$intercept/slope; k_2 = slope^2/intercept; h = intercept

3.7. Langmuir isotherm—four types

The Langmuir model was originally developed to represent monolayer sorption on a set of distinct localized sorption sites. It gives uniform energies of monolayer sorption onto sorbent surface with no transmigration of sorbate in the plane of the surface. There are no interaction between sorbed molecules, no steric hindarance between sorbed molecules and incoming ions. It is represented as [40]

$$q_e = \frac{q_m K_L C_e}{1 + K_L C_e} \tag{16}$$

The essential characteristics of the Langmuir isotherm can be expressed in terms of dimensionless constant separation factor or equilibrium parameter, R_L, given by

$$R_L = \frac{1}{1 + K_L C_0} \tag{17}$$

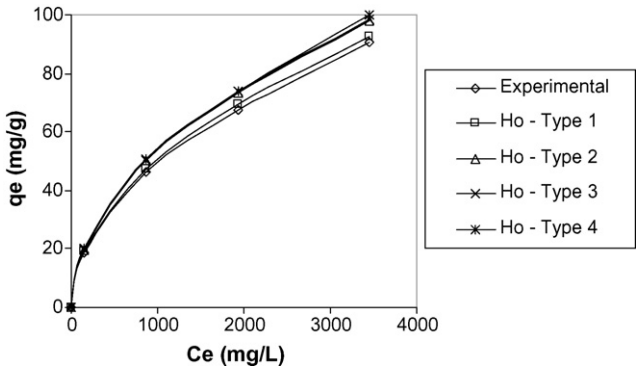

Fig. 2. Equilibrium curves for sorption of spent wash onto fly ash using Ho's pseudo-second-order isotherm (*conditions*: pH 7, dosage = 10 g, temperature = 303 K, particle size BSS# −100 + 150).

The parameter R_L indicates the shape of isotherm ($R_L > 1$ isotherm is unfavorable, $R_L = 1$ it is linear, $0 < R_L < 1$ it is favorable and $R_L = 0$ it is irreversible).

The linearized form of four types of Langmuir model is represented in Table 9. Fig. 3 represents the equilibrium data for four types of Langmuir isotherm. The evaluated Langmuir parameters were given in Table 10. Type 2 Langmuir kinetic equation is found to represent the experimental data with correlation coefficient r^2 0.996. The values of R_L are in the range of 0.032–0.436 which is less than one in the favorable region for the validity of the isotherm. However, values of non-linear error function of sum of squares and sum of absolute errors are large, hence the Langmuir isotherm is not considered as best fit model to represent the experimental equilibrium data.

3.8. Mass transfer studies

The significance of diffusion mechanisms and accurate estimates of the diffusivities inside the adsorbent particles are determined from the diffusion controlled kinetic models based on interpretation of the experimental data. The external diffusion model assumes that the concentration at the adsorbent surface tends to zero and the intraparticle diffusion is negligible at early times of contact. The external diffusion is described in the following equation called as Mathews and Weber model [41]:

$$\ln \frac{C_t}{C_0} = -k_f \frac{a}{V} t \tag{18}$$

Table 9
Langmuir isotherm kinetic model linear forms

Type	Linear form	Plot
Langmuir-1	$\frac{C_e}{q_e} = \frac{1}{K_L q_m} + \frac{C_e}{q_m}$	C_e/q_e vs. C_e
Langmuir-2	$\frac{1}{q_e} = \frac{1}{q_m} + \frac{1}{K_L q_m C_e}$	$1/q_e$ vs. $1/C_e$
Langmuir-3	$q_e = q_m - \frac{q_e}{K_L C_e}$	q_e vs. q_e/C_e
Langmuir-4	$\frac{q_e}{C_e} = K_L q_m - K_L q_e$	q_e/C_e vs. q_e

Table 8
Pseudo-second-order rate constant for the sorption of spent wash onto fly ash

Type	Parameters	293 K				303 K				313 K			
		5%	10%	15%	20%	5%	10%	15%	20%	5%	10%	15%	20%
Type 1	k_2	0.0045	0.0023	0.0013	0.0009	0.0040	0.0023	0.0011	0.0010	0.0014	0.0022	0.0012	0.0008
	h	1.8144	6.0758	7.5766	9.3985	1.6357	5.7219	6.1730	9.6939	0.9989	5.0750	6.1181	7.6266
	r^2	0.9983	0.9993	0.9992	0.9977	0.9983	0.9993	0.9988	0.9988	0.9852	0.9989	0.9964	0.9975
Type 2	k_2	0.0057	0.0027	0.0014	0.0012	0.0051	0.0027	0.0029	0.0012	0.0059	0.0027	0.0011	0.0012
	h	2.2520	7.0110	8.0789	12.164	1.9782	6.5423	7.0138	11.356	2.0417	6.1032	5.8738	9.8620
	r^2	0.9274	0.9458	0.9656	0.9088	0.9387	0.9521	0.9521	0.9280	0.9268	0.9139	0.9328	0.9009
Type 3	k_2	0.0056	0.0027	0.0014	0.0012	0.0050	0.0027	0.0013	0.0012	0.0058	0.0027	0.0011	0.0011
	h	2.2181	6.9428	8.0172	11.976	1.9477	6.4780	6.9289	11.237	2.0175	6.0410	5.9017	9.7018
	r^2	0.9022	0.9317	0.9526	0.8777	0.9143	0.9387	0.9336	0.9080	0.9045	0.8934	0.8884	0.8678
Type 4	k_2	0.0050	0.0025	0.0014	0.0010	0.0045	0.0025	0.0012	0.0011	0.0051	0.0024	0.0010	0.0010
	h	2.0261	6.5146	7.6819	10.662	1.8021	6.1205	6.5291	10.317	1.8478	5.4625	5.3405	8.5728
	r^2	0.902	0.9317	0.9526	0.8771	0.9143	0.9387	0.9336	0.9080	0.9045	0.8934	0.8884	0.8678

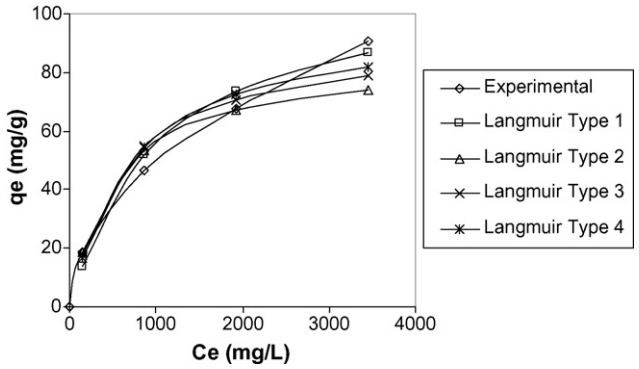

Fig. 3. Equilibrium curves for sorption of spent wash onto fly ash using Langmuir isotherm (*conditions*: pH 7, dosage = 10 g, temperature = 303 K, particle size BSS# −100 + 150).

$$\frac{a}{V} = \frac{6M}{\rho d} \tag{19}$$

By plotting $\ln(C_t/C_0)$ against t, the initial external mass transfer coefficient, k_f can be determined.

An alternative method referred to as Furusawa and Smith model [42] used to calculate the external mass transfer coefficient. It is presented as follows:

$$\ln\left[\frac{C_b}{C_o} - \frac{1}{1+m_sK_L}\right] = \ln\left[\frac{m_sK_L}{1+m_sK_L}\right] - \left[\left(\frac{m_sK_L}{1+m_sK_L}\right)k_fS_at\right] \tag{20}$$

which can be rearranged as

$$\left(\frac{1}{1+(1/m_sK_L)}\right)\ln\left(\frac{C_t}{C_0} - \frac{1}{m_sK_L}\left(1-\left(\frac{C_t}{C_0}\right)\right)\right) = -k_fS_at \tag{21}$$

The linear plot of this equation can be used to determine external mass transfer coefficient.

Pore and surface mass diffusion is governed by Fick's law and intraparticle diffusion, D. The sum of pore and surface diffusion may be calculated from the following equation [43]:

$$-\log\left(1-\left(\frac{q_t}{q_e}\right)^2\right) = \frac{4\Pi Dt}{2.303d^2} \tag{22}$$

Once the external and internal diffusion coefficients are determined for a given adsorption system, the Biot number can then be estimated from the following equation:

$$B_N = k_f\frac{d}{D} \tag{23}$$

The Biot number gives a criterion for the predominance of surface diffusion against external diffusion. Adsorption process is mainly controlled by internal diffusion mechanism where the Biot

Table 10
Langmuir isotherm parameters and correlation coefficients

Type	Parameters	293 K	303 K	313 K
Type 1	K_L (L mg^{-1})	0.001218	0.000993	0.000647
	q_m (mg g^{-1})	113.5989	111.9863	117.6726
	r^2	0.958063	0.963881	0.980157
Type 2	K_L (L mg^{-1})	0.002356	0.001938	0.000923
	q_m (mg g^{-1})	87.64105	85.29245	98.45103
	r^2	0.989293	0.987442	0.996471
Type 3	K_L (L mg^{-1})	0.002047	0.001678	0.000821
	q_m (mg g^{-1})	94.58656	92.30272	105.3924
	r^2	0.85483	0.851345	0.935686
Type 4	K_L (L mg^{-1})	0.00175	0.001429	0.000768
	q_m (mg g^{-1})	100.8575	98.68117	108.962
	r^2	0.85483	0.851345	0.935686

Table 11
Mass transfer coefficients and Biot number calculations

Dilution (%)	External mass transfer coefficient, k_f, Mathews and Weber model ($\times10^{-5}$ cm min^{-1})			External mass transfer coefficient, k_f, Furusawa and Smith model ($\times10^{-5}$ cm min^{-1})			Internal mass transfer coefficient, D ($\times10^{-7}$ cm^2 min^{-1})			Biot number, B_N using Mathews and Weber			Biot number, B_N using Furusawa and Smith		
	293 K	303 K	313 K	293 K	303 K	313 K	293 K	303 K	313 K	293 K	303 K	313 K	293 K	303 K	313 K
5	2.845	2.624	1.766	4.877	4.464	4.219	2.248	2.409	3.078	1.619	1.394	0.734	2.776	2.372	1.754
10	1.431	1.200	1.069	1.805	1.504	1.663	3.200	3.191	3.167	0.572	0.481	0.432	0.721	0.603	0.672
15	1.042	1.059	0.096	1.188	1.223	1.263	3.982	3.170	2.180	0.334	0.427	0.563	0.382	0.493	0.741
20	0.085	0.074	0.071	0.095	0.082	0.089	1.765	3.282	2.069	0.621	0.288	0.444	0.691	0.323	0.550

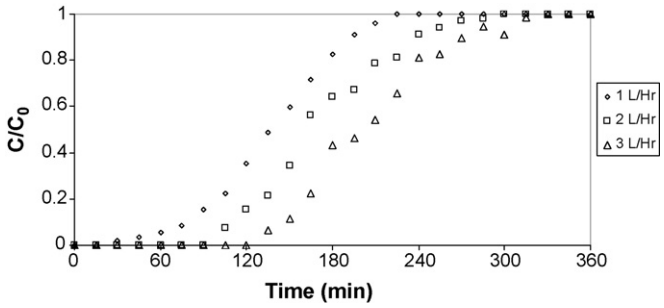

Fig. 4. Breakthrough curves for continuous sorption of spent wash onto fly ash at different flow rates (*conditions*: pH 7, dilution = 5%, particle size BSS# −100 + 150, bed height = 10 cm).

number is greater than 100 and the adsorption process is controlled by film transfer if Biot number is less than 100 [44].

The external mass transfer coefficients calculated using Mathews and Weber model and Furusawa and Smith model along with internal mass transfer coefficients and the corresponding Biot number are presented in Table 11. The Biot number values calculated using both Mathews and Weber and Furusawa and Smith are less than 100 indicating control of adsorption of spent wash onto fly ash by external film coefficients.

3.9. Packed bed models for adsorption at different flow rates

The concentration versus time profile is represented as break through curves at different flow rates. Fig. 4 provides the break through curves for sorption of spent wash onto fly ash at different flow rates. The Thomas model is widely used to study the column performance for adsorption process. The Thomas model assumes Langmuir kinetics of adsorption and no axial dispersion and that the rate driving force obeys second order reversible reaction kinetics. The model is represented as [45]

$$\frac{C}{C_0} = \frac{1}{1 + \exp[(K_{Th}/Q)(q_0 M - C_0 V_{eff})]} \tag{24}$$

The linearized form represented by

$$\ln\left(\frac{C_0}{C}\right) = \frac{K_{Th} q_0 M}{Q} - \frac{K_{Th} C_0 V_{eff}}{Q} \tag{25}$$

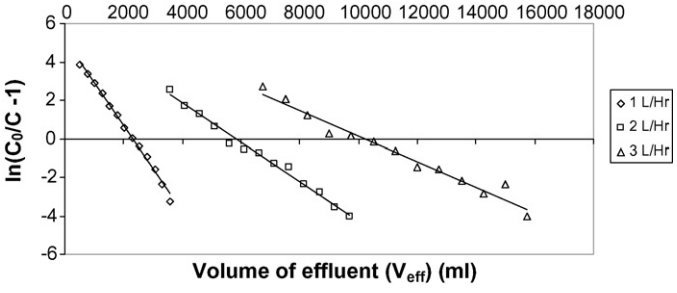

Fig. 5. Thomas model for continuous model of sorption of spent wash onto fly ash at different flow rates.

Table 12
Thomas model for the continuous sorption of spent wash

Flow rate (mL min^{-1})	Equilibrium specific uptake of spent wash solids, q_0 (mg g^{-1})	Kinetic constant in the Thomas model, K_{Th} (mL/(mg min))	r^2
17	209.294	0.0190	0.994
34	528.301	0.0172	0.988
50	930.825	0.0166	0.967

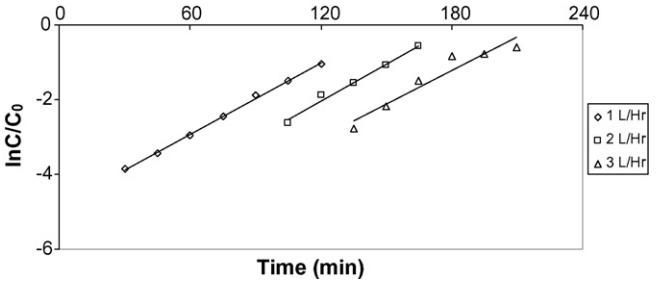

Fig. 6. Adams–Bohart model for continuous sorption of spent ash onto fly ash at different flow rates.

Table 13
Adams–Bohart model for the continuous sorption of spent wash

Flow rate (mL min^{-1})	Kinetic constant, K_{AB} (mL/(mg min))	Saturation concentration, N_0 (mg L^{-1})	r^2
17	0.0159	298.122	0.998
34	0.0164	714.655	0.986
50	0.0149	1275.775	0.920

Effluent volume is calculated from the following equation:

$$V_{eff} = Q t_{total} \tag{26}$$

$$\ln\left(\frac{C_0}{C}\right) = \frac{K_{Th} q_0 M}{Q} - (K_{Th} C_0 t_{total}) \tag{27}$$

The K_{Th} and q_0 are calculated from the slopes and intercepts obtained from Fig. 5 and are tabulated in Table 12. The linearized Thomas equation adequately describes the experimental break through sorption data as evident from the values obtained by the model.

The Adam–Bohart model is used for the description of the initial part of breakthrough curve. This model assumes that the adsorption rate is proportional to both the residual capacity of the sorbent and the concentration of the sorbing species [45].

$$\ln\frac{C}{C_0} = K_{AB} C_0 t - \frac{K_{AB} N_0 Z}{U_0} \tag{28}$$

From the plot of $\ln C/C_0$ against time at a given bed height and flow rate values describing the characteristic operational parameters of the column can be determined.

The Adams–Bohart sorption model is applied to the continuous sorption of spent wash onto fly ash in the packed bed column for the description of initial part of breakthrough curve using the experimental data. A linear relationship between $\ln C/C_0$ and t was obtained for the initial part of the breakthrough curve up to 50% breakthrough for all bed heights and is shown in Fig. 6. The values of saturation concentration (N_0) and kinetic constant of Adams–Bohart model (K_{AB}) calculated were tabulated in Table 13. The break through capacity at different flow rates was 298 mg L^{-1}, 715 mg L^{-1} and 1275 mg L^{-1} for 17 mL min^{-1}, 34 mL min^{-1} and 50 mL min^{-1}. This provides that as the flow rate increases break through capacity increases, which may be attributed to increase in flow rate results with decrease in residence time.

4. Conclusion

The sorption data for adsorption of spent wash onto fly ash was found to fit the Sips, Redlich–Peterson and Ho's pseudo-second-order type 1 isotherms model based on non-linear error functions analyzed. The sorption process was found to be controlled by external film coefficient as the Biot number was less than 100. The Thomas model was found to represent the continuous sorption for

different flow rate of studies. Adams–Bohart model was found to represent the initial part of the breakthrough curve.

References

[1] B.L. Wedzicha, M.T. Kaputo, Melanoidins from glucose and glycine: composition, characteristics and reactivity towards sulphite ion, Food Chem. 43 (1992) 359–367.
[2] V. Kumar, L. Wati, P. Nigam, I.M. Banat, B.S. Yadav, D. Singh, R. Marchant, Decolorization and biodegradation of anaerobically digested sugarcane molasses spent wash effluent from biomethanation plants by white rot fungi, Process Biochem. 33 (1) (1998) 83–88.
[3] P. Manisankar, C. Rani, S. Viswanathan, Effects of halides in the electro chemical treatment of distillery effluent, Chemosphere 57 (8) (2004) 961–966.
[4] D. Francisca Kalavathi, L. Uma, G. Subramanian, Degradation and metabolization of the pigment-melanoidin in distillery effluent by the marine cyanobacterium *Oscillatoria boryana* BDU 92181, Enzyme Microb. Technol. 29 (2001) 246–251.
[5] S. Ohmomo, Y. Kancko, S. Sirianuntapiboon, P. Somchai, P. Atthasampunna, I. Nakamura, Decolorization of molasses wastewater by a thermophileic strain, *Aspergillus fumigatus* G-2-6, Agrie Biol. Chem. 51 (1987) 3339–3346.
[6] V. Kumar, L. Wait, F. Fitzgibbon, P. Nigam, I.M. Bansat, D. Singh, R. Marchant, Bioremediation and decolorization of anaerobically digested distillery spent wash, Biotechnol. Lett. 19 (1997) 285–289.
[7] A.P. Thakkar, V.S. Dhamankar, B.P. Kapadnis, Biocatalytic decolourisation of molasses by *Phanerochaete chrysosporium*, Bioresour. Technol. 97 (1988) 1377–1381.
[8] G. Christoskovas, L.D. Lazarov, Electrochemical method for purification and discoloration of cellulose paper industry wastewaters, Environ. Prot. Eng. 14 (3/4) (2006) 69–76.
[9] P. Manisankar, S. Viswanathan, C. Rani, Electrochemical treatment of distillery effluent using catalytic anodes, Green Chem. 5 (2003) 270–274.
[10] P.K. Chaudhari, I.M. Mishra, S. Chand, Decolorization and removal of chemical oxygen demand (COD) with energy recovery: treatment of biodigester effluent of a molasses-based alcohol distillery using inorganic coagulants, Colloids Surf. A 296 (2007) 238–247.
[11] V.P. Migo, M. Matsumure, E.J.D. Rosarto, H. Kataka, Decolouration of molasses wastewater using an inorganic coagulates, J. Ferment. Bioeng. 75 (6) (1993) 438–442.
[12] S. Sinha, Y. Yoon, G. Amy, J. Yoon, Determining the effectiveness of conventional and alternative coagulants through effective characterization schemes, Chemosphere 57 (2004) 1115–1122.
[13] J.E. Van Benschoten, J.K. Edzwald, Measuring aluminum during water treatments, J. Am. Water Works Assoc. 82 (1990) 71–78.
[14] Z. Song, C.J. Williams, R.G.J. Edyvean, Treatment of tannery wastewater by chemical coagulation, Desalination 164 (2004) 249–259.
[15] R.G. Miller, F.C. Kopfler, K.C. Kelty, J.A. Stober, N.S. Ulmer, The occurrence of aluminum in drinking water, J. Am. Water Works Assoc. 76 (1984) 84–91.
[16] F.B. Dilek, S. Bese, Treatment of pulping effluents by using alum and clay-color removal and sludge characteristics, Water SA 27 (3) (2001).
[17] M.L. Hall, W.R. Livingston, Fly ash quality, past, present and future, and the effect of ash on the development of novel products, J. Chem. Technol. Biotechnol. 77 (2002) 234–239.
[18] V.S. Mane, I.D. Mall, V.C. Srivastava, Use of bagasse fly ash as an adsorbent for the removal of brilliant green dye from aqueous solutions, Dyes Pigments 73 (2007) 269–278.
[19] S. Wang, Y. Boyjoo, A. Choueib, A comparative study of dye removal using fly ash treated by different methods, Chemosphere 60 (2005) 1401–1407.
[20] K.V. Kumar, V. Ramamurthi, S. Sivanesan, Modeling the mechanism involved during the sorption of methylene blue onto fly ash, J. Colloid Interface Sci. 284 (2005) 14–21.
[21] S. Kara, C. Aydiner, E. Demirbas, M. Kobya, N. Dizge, Modeling the effects of adsorbent dose and particle size on the adsorption of reactive textile dyes by fly ash, Desalination 212 (2007) 282–293.
[22] V. Ponnusami, V. Krithika, R. Madhuram, S.N. Srivastava, Biosorption of reactive dye using acid treated rice husk: factorial design analysis, J. Hazard. Mater. 142 (2007) 397–403.
[23] S.D. Khattri, M.K. Singh, Color removal from dye wastewater using sugar cane dust as an adsorbent, Adsorpt. Sci. Technol. 17 (4) (1999) 269–282.
[24] G. McKay, E.I. Geundi, M.M. Nasser, Equilibrium studies during the removal of dyestuff from aqueous solutions using bagasse pith, Water Res. 21 (1987) 1513–1518.
[25] W.R. Knocke, L.H. Hemphill, Mercury(II) sorption of waste rubber, Water Res. 15 (1981) 275–282.
[26] A.G. Rowley, A. Cunningham, F.M. Husband, Mechanisms of metal adsorption from aqueous solutions by waste tyre rubber, Water Res. 18 (1984) 981–984.
[27] APHA, Standard Methods for the Examination of Water and Wastewater, 20th ed., American Public Health Association, American Water Works Association and Water Pollution Control Federation, Washington, DC, 1998.
[28] C. Raghukumar, G. Rivonkar, Decolorization of molasses spent wash by the white rot fungus *Flavodon flavus*, isolated from a marine habitat, Appl. Microbiol. Biotechnol. 55 (2001) 510–514.
[29] Y.S. Ho, J.F. Porter, G. McKay, Equilibrium isotherm studies for the sorption of divalent metal ions onto peat: copper, nickel and lead single component systems, Water Air Soil Poll. 141 (2002) 1–33.
[30] A. Jumasiah, T.G. Chuah, J. Gimbon, T.S.Y. Choong, I. Azni, Adsorption of basic dye onto palm kernel shell activated carbon sorption equilibrium and kinetic studies, Desalination 186 (2005) 57–64.
[31] C.K. Dany, C.W. Cheung, K.K.H. Choy, J.F. Porter, G. McKay, Sorption equilibria of metal ions on bone char, Chemosphere 54 (2004) 273–281.
[32] S.H. Chien, W.R. Clayton, Application of Elvoich equation to the kinetics of phosphate release and sorption in soil, J. Am. Soil Sci. Soc. 44 (1980) 265–268.
[33] M.J.D. Low, Kinetics of chemisorption of gases on solids, Chem. Rev. 60 (1960) 267–317.
[34] M.M. Dubinin, L.V. Radushkevich, The equation of the characteristic curve of the activated charcoal, Proc. Acad. Sci. USSR Phys. Chem. Sec. 55 (1947) 331–337.
[35] J. Li, C.J. Weaarth, Modeling sorption isotherms of volatile organic chemical mixtures in model and natural solids, Environ. Toxicol. Chem. 21 (2002) 1377–1383.
[36] J.P. Hobson, Physical adsorption isotherms extending from ultra high vacuum to vapor pressure, J. Phys. Chem. 73 (1969) 2720–2727.
[37] K. Vasanth Kumar, S. Sivanesan, Isotherms for malachite green onto rubber wood (*Hevea brasiliensis*) sawdust: comparison of linear and non-linear methods, Dyes Pigments 72 (2007) 124–129.
[38] Y.S. Ho, G. McKay, The kinetics of sorption of divalent metal ions onto sphagnum moss peat, Water Res. 34 (3) (2000) 735–742.
[39] Y.S. Ho, Second order kinetic model for the sorption of cadmium onto tree fern: a comparison of linear and non-linear methods, Water Res. 40 (2006) 119–125.
[40] I. Langmuir, The adsorption of gases on plane surface of glass, mica and platinum, J. Am. Chem. Soc. 40 (1916) 1361–1368.
[41] M.T. Sulak, E. Demirbas, M. Kobya, Removal of astrazon yellow 7GL from aqueous solutions by adsorption onto wheat bran, Bioresour. Technol. 98 (2007) 2590–2598.
[42] K.K.H. Choy, C.K. Danny, C.W. Cheung, J.F. Porter, G. McKay, Film and intraparticle mass transfer during the adsorption of metal ions onto bone char, J. Colloid Interface Sci. 271 (2004) 284–295.
[43] T. Vermeulen, Theory for irreversible and constant pattern solid diffusion, Ind. Eng. Chem. 45 (8) (1953) 1664–1670.
[44] E. Guibal, C. Milot, J.M. Tobin, Metal anion sorption by chitosan beads: equilibrium and kinetic studies, Ind. Eng. Chem. Res. 37 (1998) 1454–1463.
[45] B. Preetha, T. Viruthagiri, Batch and continuous biosorption of chromium(VI) by *Rhizopus arrhizus*, Sep. Purif. Technol. 57 (2007) 126–133.